

# Biophysical Regulation of Composite Musculoskeletal Tissue Regeneration

Catherine Nguyen<sup>1</sup>, Cole A. DeForest<sup>1</sup>, Feini Qu<sup>1</sup>

<sup>1</sup>University of Washington, Seattle WA  
feiniqu@uw.edu

**Disclosures:** C. Nguyen (N), C.A. DeForest (N), F. Qu (N)

**INTRODUCTION:** Regeneration of composite musculoskeletal tissues (e.g., limbs) after injury or resection is limited in mammalian species, often resulting in fibrotic scarring instead of regrowth. To this end, we study the murine digit tip, which fully regenerates after distal amputation via the activation of local stem/progenitor cells (the “blastema”), but scars after more proximal amputations [1,2]. While it is known that mechanical cues in the environment modulate scar formation [3,4] and tissue regrowth [5,6], it remains unclear how the wound’s intrinsic mechanical properties may affect blastema formation and regenerative capacity after digit amputation. We hypothesized that pro-regenerative blastema cell behaviors such as proliferation, migration, and differentiation are dependent on the emergent biophysical properties of the extracellular matrix (ECM). To test this hypothesis, we first sought to quantify the stiffness and structure of the wound microenvironment following level-dependent digit amputation.

**METHODS:** Mouse model: Bilateral distal (regenerative) and proximal (non-regenerative) digit amputations were performed on the hindlimb terminal (P3) and middle (P2) phalanges of 10-week-old C57BL/6 male and female mice, respectively, with IACUC approval (n = 3 mice/group/timepoint). We quantified bone length and volume via *in vivo* micro-computed tomography ( $\mu$ CT; 10.5  $\mu$ m resolution, SCANCO VivaCT 40) pre- and post-surgery at 0 days post-amputation (DPA) and at 7, 10, 14, and 21 DPA (n = 6 digits/group/timepoint). Harvested digits were either embedded in optimal cutting temperature compound for cryosectioning or fixed and processed for histology. Matrix evaluation: Paraffinized sections (5  $\mu$ m thickness) of 14 DPA digits were stained with hematoxylin & eosin (H&E) and picrosirius red (PSR) and imaged with brightfield and/or polarized light microscopy. The open-source program MatFiber [7] was used to visualize collagen alignment at the wound site of PSR-stained sections. Next, we measured the stiffness of the P3 blastema or P2 scar tissue using an atomic force microscope (AFM; Asylum Cypher ES) [8]. Fresh frozen sections (35  $\mu$ m thickness) of 21 DPA digits underwent force spectroscopy (n = 3 samples/group) in HEPES buffer using a spherical probe (NanoAndMore,  $\phi$  = 10.8  $\mu$ m, k = 0.08 N/m). The average ECM stiffness (Young’s elastic modulus) of each sample was determined using a minimum of 10 force curves acquired at distinct locations and fitted with the Hertz model [9]. Statistical significance between groups was determined by 2-way ANOVA with Tukey’s post-hoc test or by a 2-tailed unpaired Student’s t-test (p  $\leq$  0.05).

**RESULTS:** Our  $\mu$ CT results indicated that ~22% of the P3 length was removed with distal amputation, whereas ~39% of the P2 length was removed with proximal amputation (Fig. 1). As expected, bone remodeling and regeneration occurred after P3, but not P2, amputation. The P3 bone underwent degradation within 10 to 14 DPA and subsequent outgrowth by 21 DPA (Fig. 1A), with concomitant changes in bone length and volume (Figs. 1B and 1C, p  $\leq$  0.05). Conversely, the P2 bone did not exhibit changes in length or volume after amputation (Fig. 1, p > 0.05), instead forming a bony callus and fibrotic scar by 14 DPA (Figs. 1A and 2). The P2 scar was distinguished by increased collagen density and alignment compared to the P3 blastema (Figs. 2B and 2C). Interestingly, histology showed that areas of high cell density primarily occurred in regions with minimal collagen deposition (Figs. 2 and 3A). Force spectroscopy revealed that the average stiffness of the P2 scar (4.4  $\pm$  1.1 kPa) was approximately twice as much as the P3 blastema (1.8  $\pm$  0.7 kPa) (Fig. 3B, p  $\leq$  0.05).

**DISCUSSION:** Our findings suggest that the regenerative capacity of the amputated digit tip is correlated with emergent properties of the wound microenvironment, including ECM stiffness and structure. Blastema formation and P3 bone regrowth readily occurred in a compliant matrix with minimal collagen deposition. Conversely, osteogenesis distal to the P2 bone stump was not observed despite callus formation, indicating that the dense and highly aligned collagen scar may have physically inhibited cell proliferation and tissue outgrowth. In addition, a stiffer ECM may alter cellular mechanosensing, directing cells towards a myofibroblast phenotype that perpetuates scar formation [4]. A recent study found that increasing the hyaluronic acid content of the digit ECM is associated with decreased tissue stiffness and improved P2 regeneration [6], which highlights the therapeutic potential of altering local matrix properties. To decouple biochemical and mechanical cell-matrix interactions, we are currently developing a tunable three-dimensional hydrogel platform [9] that recapitulates the dynamic biophysical properties of the digit microenvironment after amputation. Future work will use this *in vitro* system to investigate how modulating substrate stiffness over time affects stem/progenitor cell activation and behavior, laying the foundation for novel strategies that promote the regeneration of limbs following injury or resection.

**SIGNIFICANCE:** Limb loss affects an estimated 2 million Americans, with prostheses ultimately failing to replicate the structure and function of the original tissues. Therefore, the ability to regrow the missing limb will significantly improve patient outcomes.

**REFERENCES:** [1] Storer+, Dev Cell 2020. [2] Qu+, FASEB J 2020. [3] Chen+, Nat Commun 2021. [4] Hinz+, Periodontol 2013. [5] Qu+, Biomaterials 2016. [6] Mui+, bioRxiv 2024. [7] Fomovsky & Holmes, Am J Physiol Heart Circ Physiol 2010. [8] Li+, Acta Biomater 2017. [9] Kopyeva+, Adv Mater 2024.

**ACKNOWLEDGEMENTS:** This work was supported by funds from the NIH (4R00HD105203) and from the UW, including OAW (3Rs Pilot Funding), ISCRM (Fellows Program), and the Dept. of Mechanical Engineering. Part of this work was conducted at UW’s Molecular Analysis Facility.

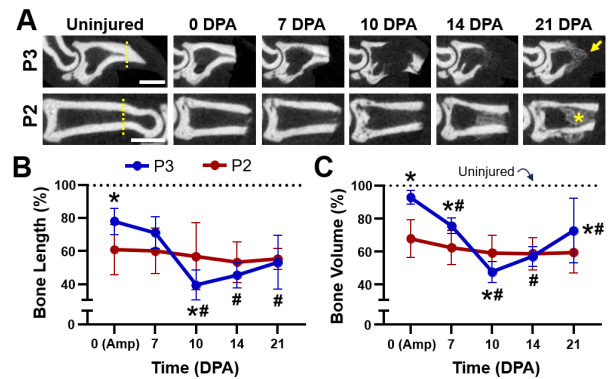


**Fig. 1.** (A)  $\mu$ CT images show bone remodeling and regrowth (arrow) after P3 amputation and callus formation (asterisk) after P2 amputation. Dotted line indicates amputation plane. Scale bars = 500  $\mu$ m. (B) Bone length and (C) volume over time (% of uninjured) after digit amputation (n = 6 digits/group/timepoint, mean  $\pm$  SD). \* = p  $\leq$  0.05 vs. P2, # = p  $\leq$  0.05 vs. 0 DPA (Amp).

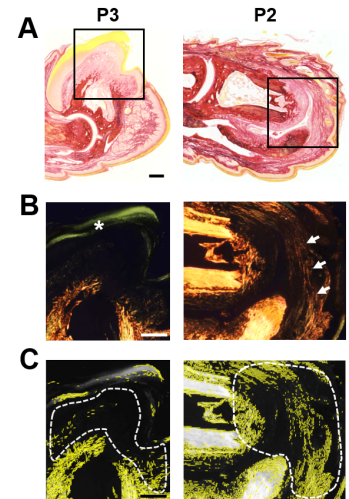


**Fig. 2.** (A) Mid-sagittal digit sections at 14 DPA stained with PSR. Box indicates magnified region in (B). (B) PSR-stained sections viewed under polarized light reveal collagen fibers (arrows) in the P2 scar but not the P3 blastema. Asterisk indicates nail. (C) Collagen alignment (yellow vectors) within blastema and scar regions (dashed line). Scale bars = 200  $\mu$ m.

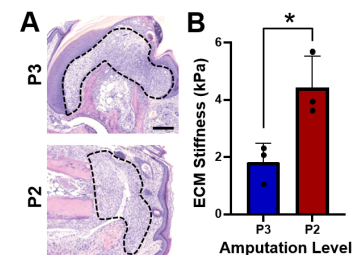


**Fig. 3.** (A) H&E staining of digit sections showing the target regions for force spectroscopy (dashed outline). Scale bar = 200  $\mu$ m. (B) ECM stiffness of the P3 blastema and P2 scar at 21 DPA (n = 3 samples/group, mean  $\pm$  SD). \* = p  $\leq$  0.05 between groups.